CHARM IN DIFFRACTIVE DEEP INELASTIC SCATTERING*

Nikolai Vlasov

Nuclear Physics Institute, Moscow State University, 119 899 Moscow, Russia
e-mail: vlasov@mail.desy.de

(Received June 7, 2002)

Diffractive production of $D^{*\pm}(2010)$ mesons in deep inelastic scattering has been studied with the ZEUS detector at HERA using an integrated luminosity of $82\,\mathrm{pb}^{-1}$. Diffractive events were identified by the presence of a large rapidity gap in the final state. The $D^{*\pm}$ mesons were reconstructed in the decay channel $D^{*+} \to D^0\pi_s^+$ with $D^0 \to K^-\pi^+$(+c.c.). Differential cross sections were measured in the kinematic region $Q^2 > 1.5\,\mathrm{GeV}^2$, $0.02 < y < 0.7$, $x_{\mathbb{P}} < 0.035$, $\beta < 0.8$, $P_{\mathrm{T}}^{D^*} > 1.5\,\mathrm{GeV}$ and $|\eta^{D^*}| < 1.5$. The measured integrated and differential cross sections are compared with theoretical predictions.

PACS numbers: 12.38.Aw, 12.38.Bx

1. Introduction

There are several different theoretical models for describing diffractive interactions. The so-called "Resolved Pomeron" model [1, 2] predicts unsuppressed charm production compared to light flavour production if the Pomeron is gluon-dominated. In the two-gluon exchange models [3,4] charm production is suppressed at leading order but it can be enhanced by the inclusion of the real and virtual gluon corrections. Thus charm production in diffractive interactions provides a probe of the underlying dynamics of the diffractive exchange.

The analysis presented in this note was performed with the data taken by the ZEUS Collaboration from 1998 to 2000. This data set corresponds to an integrated luminosity of $82\,\mathrm{pb}^{-1}$. The standard procedure was used to identify DIS events and to reconstruct $D^{*\pm}$ mesons in their decay mode $D^{*+} \to D^0\pi_s^+$ with $D^0 \to K^-\pi^+$(+c.c.). Events with a large rapidity gap

* Presented at the X International Workshop on Deep Inelastic Scattering (DIS2002) Cracow, Poland, 30 April–4 May, 2002.

in the forward (outgoing proton) direction were selected by requiring that the pseudorapidity of the most forward energy cluster $\eta_{\max} < 3$. This leaves a sizable proton-dissociation background contribution, which was estimated to be $17 \pm 3\%$ and was subtracted from all cross sections.

2. Cross sections

The $D^{*\pm}$ mesons were reconstructed in the kinematic region $P_{\mathrm{T}}^{D^*} > 1.5\,\mathrm{GeV}$ and $|\eta^{D^*}| < 1.5$. In addition to the standard DIS kinematic variables (Q^2 and y), the diffractive variables $x_{\mathbb{P}}$ and β were used to define the kinematic region, where $x_{\mathbb{P}}$ and β are defined as the fraction of the proton's momentum carried by the Pomeron and the fraction of the Pomeron's momentum carried by the struck quark, respectively. In the kinematic region defined by $1.5 < Q^2 < 200\,\mathrm{GeV}^2$, $0.02 < y < 0.7$, $x_{\mathbb{P}} < 0.035$, $\beta < 0.8$, $P_{\mathrm{T}}^{D^*} > 1.5\,\mathrm{GeV}$ and $|\eta^{D^*}| < 1.5$ the cross section was measured to be

$$\sigma_{e^+p\to e^+D^{*\pm}Xp} = 505 \pm 43(\mathrm{stat})^{+30}_{-61}(\mathrm{syst})^{+21}_{-21}(\mathrm{p.diss.})\,\mathrm{pb}\,. \qquad (1)$$

Three models are compared to the measured cross sections:

(1) the resolved Pomeron model, as implemented in the fits to HERA data made by Alvero *et al.* (ACTW) [2],

(2) the two-gluon exchange "saturation" model of Golec-Biernat and Wusthoff [5], as implemented in the SATRAP MC generator interfaced to RAPGAP [6] and

(3) the two-gluon exchange model of Bartels *et al.* (BJLW) [3], which is also implemented in the RAPGAP MC generator. Although the SATRAP and BJLW predictions are both based on two-gluon exchange, they differ in the treatment of the $q\bar{q}g$ final state which is an important contributor to charm production.

The ACTW NLO QCD prediction was calculated assuming a charm mass of $m_c = 1.45\,\mathrm{GeV}$ and the Peterson fragmentation function (with $\varepsilon = 0.035$) for charm decay. The probability for charm to fragment into a $D^{*\pm}$ meson was taken as 0.235 [7] and the renormalisation and factorisation scales as $\mu_{\mathrm{R}}^2 = \mu_{\mathrm{F}}^2 = Q^2 + 4m_c^2$. The predicted cross section from fit B by Alvero *et al.*, which assumes a gluon-dominated Pomeron, is favoured by data

$$\sigma^{\mathrm{ACTW,\,fitB}}_{e^+p\to e^+D^{*\pm}Xp} = 530\,\mathrm{pb}\,. \qquad (2)$$

The D^* diffractive cross section was also measured in the low $x_{\mathbb{P}}$ region ($x_{\mathbb{P}} < 0.01$) as

$$\sigma^{x_{\mathbb{P}}<0.01}_{e^+p\to e^+D^{*\pm}Xp} = 240 \pm 25(\mathrm{stat})^{+14}_{-23}(\mathrm{syst})^{+10}_{-10}(\mathrm{p.diss.})\,\mathrm{pb}. \qquad (3)$$

This cross section is compared with the two-gluon exchange models with the same parameters as in the ACTW calculations case, except that now $\mu_{\rm R}^2 = \mu_{\rm F}^2 = p_\perp^2 + 4m_c^2$. Using the proton structure function GRV-94 the predicted cross sections are:

$$\begin{aligned} {\rm BJLW} c\bar{c} : \sigma_{e^+p\to e^+D^{*\pm}Xp} &= 160\,{\rm pb}\,, & (4)\\ {\rm BJLW} c\bar{c} + c\bar{c}g : \sigma_{e^+p\to e^+D^{*\pm}Xp} &= 570\,{\rm pb}\,, & (5)\\ {\rm SATRAP} : \sigma_{e^+p\to e^+D^{*\pm}Xp} &= 250\,{\rm pb}\,. & (6)\end{aligned}$$

The BJLW $c\bar{c}$ contrubution (4) is too small, while the combination of the $c\bar{c}$ and $c\bar{c}g$ contributions (5) overestimates the data. The SATRAP prediction (6) is in good agreement with the data.

The differential cross sections for our full $x_{\mathbb{P}}$ range ($x_{\mathbb{P}} < 0.035$) are presented as a functions of $P_{\rm T}(D^*)$, $\eta(D^*)$, β, $x_{\mathbb{P}}$, $\log_{10}(M_X^2)$, $x(D^*)$, $\log_{10}(Q^2)$, W. The fractional momentum of the $D^{*\pm}$ in the γ^*p system is defined as $x(D^*) = \frac{2|p^*(D^*)|}{W}$, where $p^*(D^*)$ is the $D^{*\pm}$ momentum in the γ^*p center-of-mass frame.

Fig. 1 compares the predictions of ACTW fit B with the measured differential cross sections. The shaded band in the figure indicates the uncertainty arising from the variation of the charm mass in the calculations between 1.3

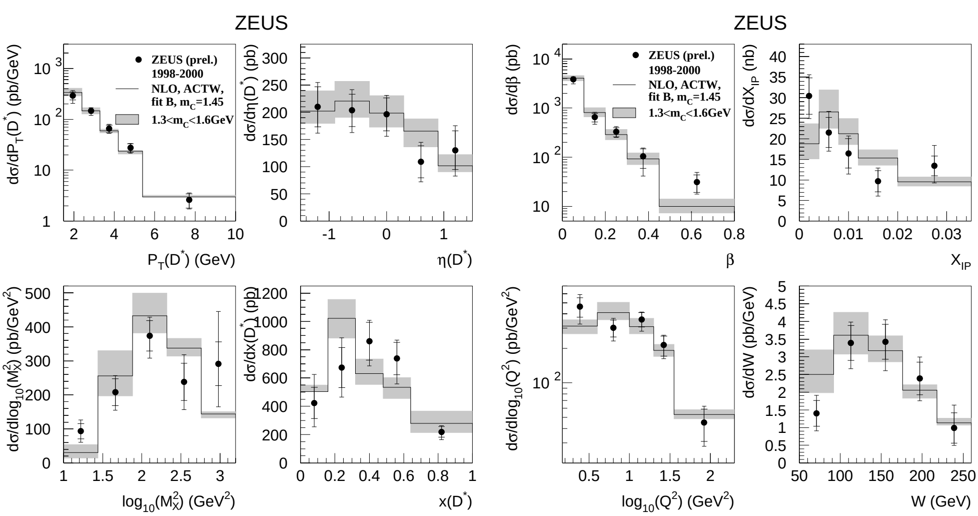

Fig. 1. Differential cross sections for $D^{*\pm}$ production in the kinematic region described in the text. The cross sections are shown as a function of $P_{\rm T}(D^*)$, $\eta(D^*)$, β, $x_{\mathbb{P}}$, $\log_{10}(M_X^2)$, $x(D^*)$, $\log_{10}(Q^2)$, W. The inner bars indicate the statistical uncertainties, while the outer ones indicates the statistical and systematic uncertainties added in quadrature. The histogram is the ACTW result. The shaded area shows the effect of varying the charm quark mass.

and 1.6 GeV. The ACTW model is in reasonable agreement with the measured differential distributions in both shape and normalisations.

Fig. 2 shows the comparisons with SATRAP, BJLW $c\bar{c}$ only and BJLW $c\bar{c}+c\bar{c}g$ predictions. The SATRAP model is in good agreement with the measured differential cross sections in both shape and normalisations. The $c\bar{c}$ contribution from the BJLW calculations clearly fails to describe the measured cross sections. The full BJLW prediction gives a reasonable description of the shapes of the distributions except $\log_{10}(M_X^2)$ and $x_{\mathbb{P}}$. These models may not be appropriate for the full $x_{\mathbb{P}}$ range.

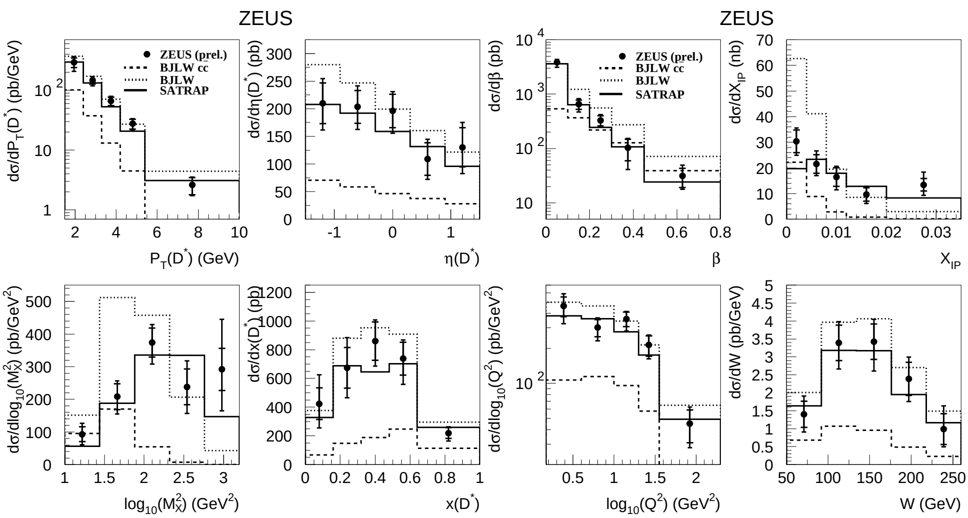

Fig. 2. Differential cross sections for $D^{*\pm}$ production in the kinematic region described in the text. The cross sections are shown as a function of $P_{\mathrm{T}}(D^*)$, $\eta(D^*)$, β, $x_{\mathbb{P}}$, $\log_{10}(M_X^2)$, $x(D^*)$, $\log_{10}(Q^2)$, W. The inner bars indicate the statistical uncertainties, while the outer ones indicates the statistical and systematic uncertainties added in quadrature. The curves correspond to the different models described in the text.

3. Ratio of diffractive to inclusive $D^{*\pm}$ production

The ratio R_D of diffractively produced $D^{*\pm}$ mesons to inclusive $D^{*\pm}$ mesons production was measured with replacement of the $x_{\mathbb{P}}$ and β requirements with $x < 0.028$ for the inclusive $D^{*\pm}$ sample

$$R_D = \frac{\sigma^{\mathrm{dif}}}{\sigma^{\mathrm{inc}}} = 6.3 \pm 0.6(\mathrm{stat})^{+0.3}_{-0.7}(\mathrm{syst})^{+0.3}_{-0.3}\,(\mathrm{p.diss.})\,. \tag{7}$$

Fig. 3 compares the measured differential ratios R_D with two Pomeron structure function parametrisations which implemented in RAPGAP: ACTW fit B and "H1 fit 2" [8]. The RAPGAP generator was also used to produce the inclusive $D^{*\pm}$ distributions using the proton structure function GRV 94.

Fig. 3 shows that there is no significant dependance of R_D from Q^2 or W. The diffractive relative contribution is larger at small $P_{\rm T}(D^*)$ and negative $\eta(D^*)$. The ACTW model agrees in both shape and normalisation, while the Pomeron parametrisation according to "H1 fit2" overestimates the absolute values of R_D.

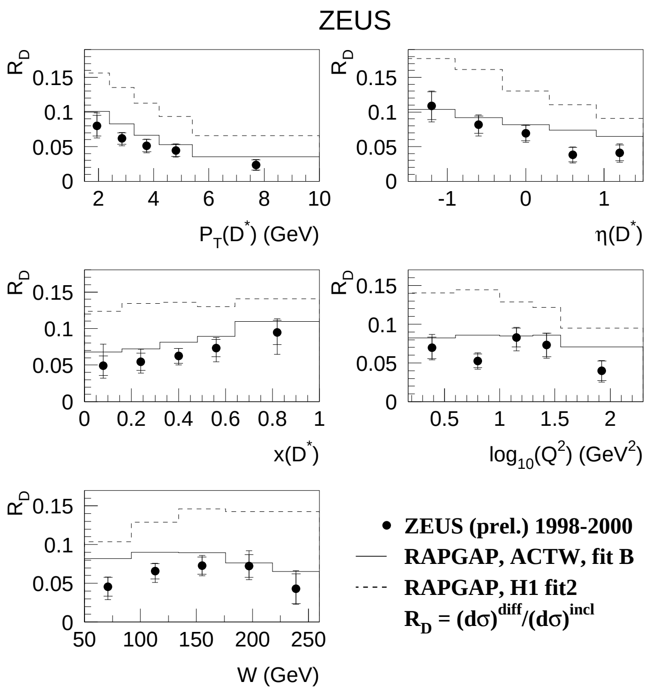

Fig. 3. The measured ratio R_D of diffractively produced $D^{*\pm}$ mesons to inclusive $D^{*\pm}$ mesons production. The ratio is shown as a function of $P_{\rm T}(D^*)$, $\eta(D^*)$, $x(D^*)$, $\log_{10}(Q^2)$, W. The inner bars indicate the statistical uncertainties, while the outer ones indicates the statistical and systematic uncertainties added in quadrature. The curves correspond to the different models described in the text.

REFERENCES

[1] G. Ingelman, P. Schlein, *Phys. Lett.* **B152**, 256 (1985); A. Donnachie, P.V. Landshoff, *Phys. Lett.* **B191**, (1987); *Nucl. Phys.* **B303**, 634 (1988).

[2] L. Alvero *et al.*, *Phys. Rev.* **D59**, 74022 (1999); `hep-ph/9806340`.

[3] J. Bartels, H. Lotter, M. Wusthoff. *Phys. Lett.* **B386**, 389 (1996); H. Lotter, *Phys. Lett.* **B406**, 171 (1997).

[4] E.M. Levin, A.D. Martin, M.G. Ryskin, T. Teubner, *Z. Phys.* **C74**, 671 (1997).

[5] K. Golec-Biernat, M. Wusthoff, *Phys. Rev.* **D59**, 014017 (1999).

[6] H. Kowalski, M. Wusthoff, "Satrap model for diffractive DIS processes", proceedings of the 8th International Workshop Deep Inelastic Scattering and QCD (2000).

[7] L. Gladilin, `hep-ex/9912064`.

[8] C. Adloff *et al.*, [H1 Collaboration], *Z. Phys.* **C76**, 613 (1997).